Active Transtensional Structures Mapped in the West of Karakoram Fault (KF), Kashmir Himalayas

Dk Nurul Azeerah Pengiran Omar[1,✉], Afroz Ahmad Shah[1], Nurhafizah Abd Manan[1]

[1] University Brunei Darussalam, Brunei Darussalam
✉ azeerahpgo@hotmail.com

Keywords: NW Himalaya, normal fault, transtension, Kashmir

1. Introduction

Over the geological past the continent-continent collision between the lithospheric plates of India and Eurasia has caused the formation, orientation, pattern, and chronology of geological structures throughout the Himalaya orogen (Yin, 2006; Stevens and Avouac, 2015; Shah, 2016; Shah and Malik 2017; Burg and Bouilhol, 2019; Shah et al., 2020). These structures have formed, and evolved differently along and across the orogen, and it is estimated that about 50 % of the ongoing convergence is mainly absorbed by the Main Himalayan Thrust (MHT), which on surface emerges as the Main Frontal Thrust (MFT) (Stevens and Avouac, 2015; Bilham, 2019). Interior faults are known to accommodate some amount of the plate convergence (Shah, 2013), but the quantitative measurements are usually missing, which is primarily because not all active faults have been studied in detail. The presence of unknown active faults (Shah et al., 2018) further complicates this story.

Broadly, the geological structures are distributed differently along and across the Himalaya and Tibet (Tapponnier and Molnar, 1977; Shah et al., 2018) which are the two major landmasses that preserve the evidence of tectonic processes like subduction, plutonism, and ongoing collision. Geologically, the Himalayan-Tibetan orogen is composed of a complex tectonic collection that preserves evidence of geological events in a chronological order from north to south (Zhao, and Xie, 1993). It includes accretion of microcontinents, flysch complexes, and island arcs, against the southern boundary of the Eurasian plate since the early Paleozoic (e.g. Yin and Harrison, 2000; Murphy et al., 2002). The tectonic topography preserves such evidence, and in particular the younger structures that have formed as a result of the ongoing collisional processes across, and along the orogen. Such structures are remarkably observable on the satellite images, and a quick glance on them reveals that a relatively narrow width of deformation zones is noticeable in NW portions of the orogen, while they are much wider in the eastern regions (Fig. 1A). This transition is marked on either side of the Karakoram fault (KF), which is the major dextral strike-slip fault and accommodates the regional oblique convergence between the two plates (Fig. 1). It defines the tectonic boundary where the western Tibetan plateau meets the Himalayan fold-and-thrust belt (Murphy et al., 2002).

Previous works have extensively produced data on the frontal portions of the Himalayas because most of the ongoing convergence is reported on the Himalayan frontal thrust system, which has also caused many larger magnitude earthquakes in the region (e.g. Bilham, 2019). The work presented here however aims to explore the regions in the west and northwest of the KF (Fig. 2). The motivation is to map the existence of what have been traditionally called out-of-sequence faulting in the NW Himalayas and to produce data on the active versus inactive nature of deformation in the interior Himalayas, and to reevaluate the earthquake geology and tectonics of the region.

2. Methodology

Satellite images have truly transformed the regional and local mapping of geological structures, and over the decades these data have been extensively useful in mapping of the structural details that were impossible to achieve on foot. This is particularly true for regional mapping exercises, which require a broader outlook (e.g. Tapponnier and Molnar, 1977, Nakata, 1989; Malik, and Nakata, 2003; Sahoo and Malik, 2017; Shah 2013; Shah et al., 2020). Additionally, regional mapping is hard to achieve during traditional geological fieldworks where limitations of time, resources, accessibility, and the fear of crossing international borders often complicates and exhausts the mapping motivations (Shah and Malik, 2017). Therefore, we take full advantage of 30 m Shuttle radar topography (SRTM) data here to map the regional geological structures. The mapping of geomorphic features was done by manually tracing topographic breaks, triangular facets, ridge crests, ruptured Holocene sedimentary deposits (e.g. alluvial fans, fluvial terraces etc.), and glacial landforms. Wherever applicable, the rule-of-V was used to mark the dip direction of bedding and faults. The moment tensor solutions are extracted from the GeoMap App

Proceedings of the 5th International YES Congress
DOI: 10.2312/yes19.12

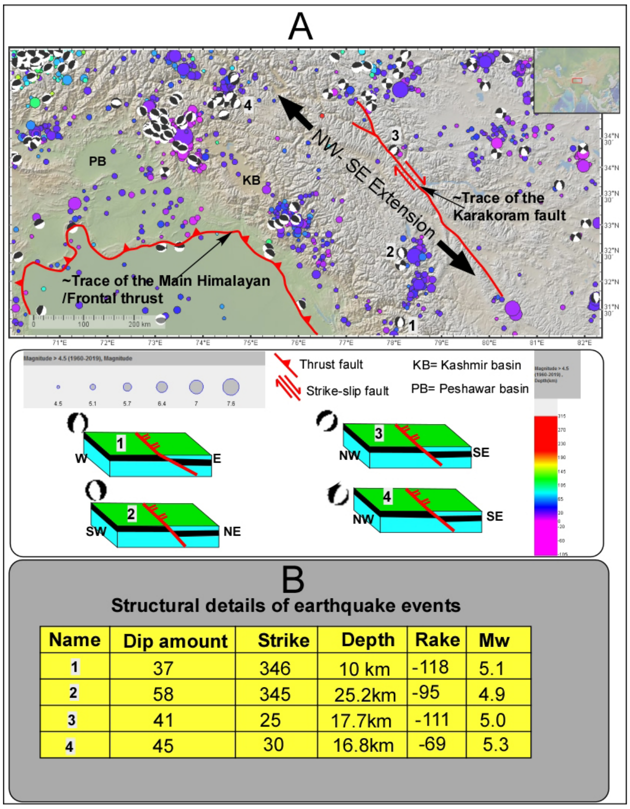

Name	Dip amount	Strike	Depth	Rake	Mw
1	37	346	10 km	-118	5.1
2	58	345	25.2km	-95	4.9
3	41	25	17.7km	-111	5.0
4	45	30	16.8km	-69	5.3

Figure 1: (A) Regional map showing the two major active faults system in NW Himalaya. The faults are in red, and the background satellite image is derived from the GeoMap App. The earthquake hypocenters (color filled circles and moment tensor solutions (earthquake beach balls)) are also plotted. The 3D-illustrations are based on the fault plane solutions that are labelled as numbers, and are interpreted as the best possible representative events of active normal faulting in the region. (B) The earthquake structural details that are used for the 3D-illustrations.

(http://www.geomapapp.org). and it covers data from January 1976 until July 2019 (Fig. 1). These data are used and correlated with our geomorphic mapping of tectonic landforms to interpret and understand the nature of faulting in the interior Himalayas.

3. Results and interpretation

3.1. Faulting

The geomorphic evidence of active normal faulting in the NW Himalayas is ubiquitous (Figs. 3 to 5). The > 60 km long and ~N-S trending normal fault is one of the most prominent looking geomorphic features in the region, and is located to the west of the Karakoram fault (Fig. 4). The ~N-S oriented elongated valley that is filled with Holocene sediments is a direct consequence of normal faulting, and it suggests a half graben geometry where the fault is dipping east (Fig. 4). The abrupt truncation of the ~NW-SE oriented ridge in front of the Tso Moriri Lake indicates faulting, which is consistent with the eastwards dipping fault plane (Fig. 4). Broadly, the region mapped here (e.g. Fig. 4) shows dominantly NW-SE, and NE-SW faults, which crosscut each other. The ridge

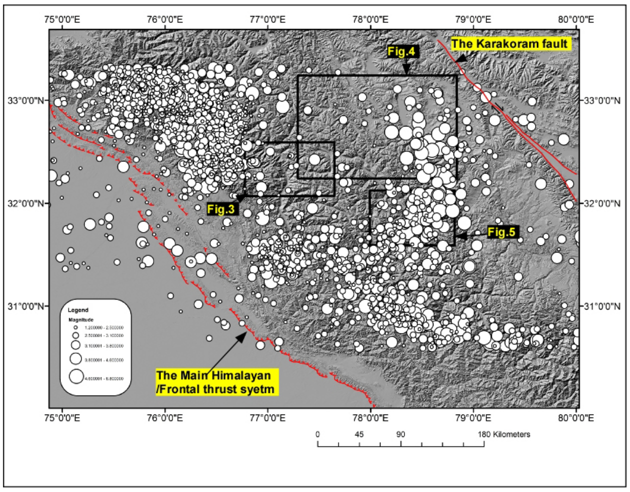

Figure 2: The shuttle radar topography (SRTM) with the regional seismicity. The major faults are shown in red, and the rectangular regions represent the areas that are studied in details (see Fig. 3 to 5).

crests are truncated by faults, triangular facets are widespread, and clear, and often Holocene filled glacial valleys are also cut by faults, which are narrow and spread across the region. This intersecting relationship of geological structures shows that ~NE-SW faults are older, and are truncated, and often cut by younger ~NW-SE faults. This suggests either the faults have formed together or, ~NW-SE trending faults are younger (see Discussion for details). Similar structures are observed in other areas (e.g. Fig. 3) where clear evidence for faults is observed, and a range of active tectonic features suggest active faulting. The entire region shows a consistent pattern of faults (Figs. 3 to 5) where a number of ~NW-SW and ~NE-SW trending normal faults are also mapped. Together all these faults show evidence of Holocene movement, and therefore these are active.

The abundance of topographic breaks that we have mapped in the region is mainly interpreted as normal faults because they are consistent with regional extension that has been observed in Tibet and Kashmir Himalaya (e.g. Shah et al., 2018). These faults are a direct consequence of the ongoing oblique convergence of India and Eurasia. The ~NW-SE major trending normal faults have displaced ~NE-SW trending normal faults, which indicate that it is younger, and our mapping shows that both are active, and interrelated to each other. Similarly, a large number of SE dipping normal faults are mapped (Figs. 3 to 5) and interpreted to have formed syn-tectonic with the oblique plate convergence that has also created the frontal thrust later in the Himalayan orogenesis. The topographic expresses of the mountains and valleys clearly show the faulting pattern, and the drainage system seems to have mirrored and followed the fault patterns. It is obvious that the entire region is split into

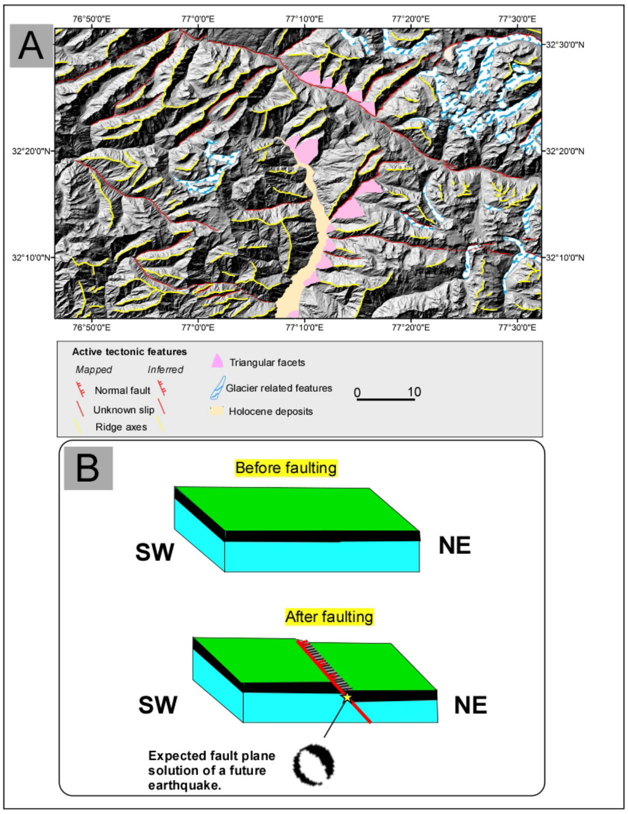

Figure 3: (A) Satellite image with interpreted tectonic and other geomorphic features. (B) 3D-illustrations before and after faulting. It is representative of one of the major normal fault systems that we have mapped here.

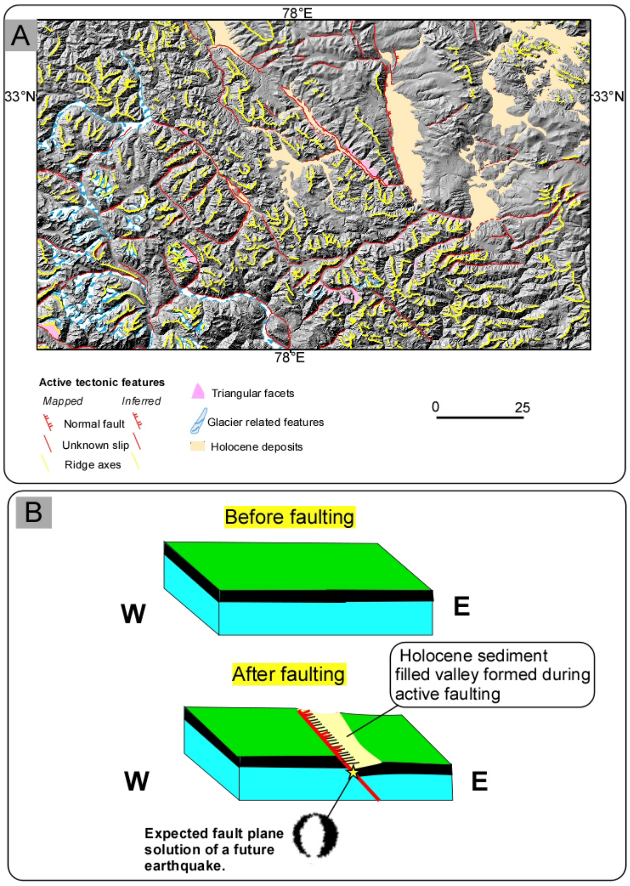

Figure 4: (A) Satellite image with interpreted tectonic and other geomorphic features. A number of syn-tectonic valleys are filled with Holocene sediments. (B) 3D illustrations before and after faulting. It is representative of one of the major normal fault systems that we have mapped here.

different ridges and valleys because of the progressive deformation that has formed these faults.

3.2. Earthquake moment tensor solutions

The distribution of earthquake hypocenters and examination of the available moment tensor solutions have corroborated with our mapping (Fig. 1A and 1B). The dominance of shallow focus earthquakes in the entire region is consistent with the brittle deformation of the interior portions. Some clusters are observed, which are mostly related to the major earthquakes events in the past. The ~NW-SE directed crustal extension that we have mapped above is also reflected from the moment tensor solutions, which show ~N-S and ~NE-SW trending normal faults. The instrumental earthquakes clearly show that normal faulting is active, and our mapping demonstrates the geomorphic and structural evidence of such events (Fig. 3 to 5). Figure 1B shows the structural parameters used to make the 3D-illustrations, which reflect the mapping of the geomorphic landform shown above.

4. Discussion

Shah et al. (2018) mapped the regional normal faults in the Kashmir Himalaya. They interpreted that ~NW-SE directed crustal extension is actively taking place in Kashmir Himalaya as well, and that it resembles the ~E-W extension that Tibet is undergoing (Fig. 6). The new mapping shown above further demonstrates that such faulting is ubiquitous throughout the west and southwest of the Karakoram fault. We have mainly observed orogen parallel faults, and ~NE-SW and ~N-S trending normal faults throughout the study area (Figs. 2 to 6). These normal faults are active, have ruptured and displaced Holocene deposits, and are morphologically similar to the normal faulting pattern that is observed in Tibet (Shah et al., 2018). The topographic expression of faulting is mainly shown by a number of faults and these are interpreted as normal faults, which have formed syn- or postgenetic to the formation of the Karakorum fault because we have observed dextral offset of normal faults at KF (Fig. 6D). The mapping further illustrates that ~NW-SE trending faults have truncated, and displaced the ~NE-SW trending faults (Figs. 2 to 5), which suggests the relative age relationship and confirms the earlier formation of ~NW-SE trending faults. The available earthquake moment tensor solutions (Fig. 1) strengthen our geomorphic mapping, and indicate the ~NW-SE to ~E-W directed crustal extension. This means on a regional scale that the ongoing lithospheric plate convergence is also absorbed by ~E-W extension, and that is strikingly similar to how Tibet is deforming

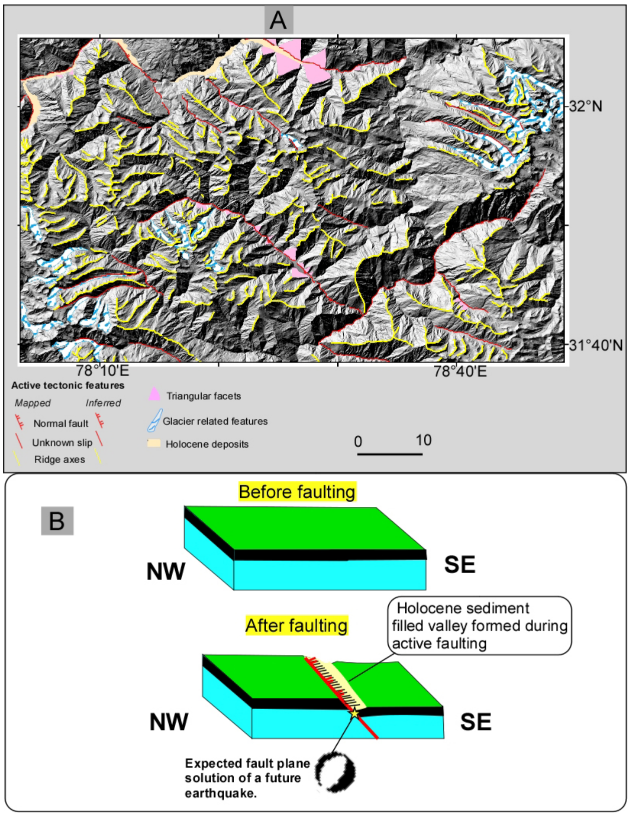

Figure 5: (A) Satellite image with interpreted tectonic and other geomorphic features. The rugged topography is dissected by glaciers, which often occupy tectonically controlled valleys. (B) 3D-illustrations before and after faulting. It is representative of one of the major normal fault systems that we have mapped here.

(McCaffrey and Nabelek 1998; Shah et al., 2018).

Further, the only major dextral strike-slip fault that exists in the NW Himalaya is the Karakoram fault (KF). The earthquake moment tensor solutions suggest (Fig. 1) that thrust faulting dominates at the frontal portions, which is consistent with the normal convergence of the two plates in convergence. However, north of Kashmir, the normal faulting predominates, and our mapping supports this with geomorphic evidence of normal faulting (Figs. 2 to 5). The faults east of KF are dominantly strike-slip and normal, and the ongoing deformation is consumed on these structures in the Tibetan plateau region (Yin and Harrison, 2000). Although the actual cause of this extension remains a controversial topic (e.g. Tapponnier and Molnar, 1977; Tapponnier et al., 1982; Yin and Harrison, 2000), our new mapping of the topographic landforms seems to suggest that regional oblique convergence can transport rocks on major strike-slip systems and could cause simultaneous extension (Fig. 6). Such a mechanism requires active and large systems of strike-slip movement in Tibet that are moving relatively faster compared to those in the east. The regional structures in NW Himalaya are broadly distributed in some restricted locations, and that suggests that frontal portions are dominated by ~NW-SE trending thrusts while interior regions are controlled by orogen

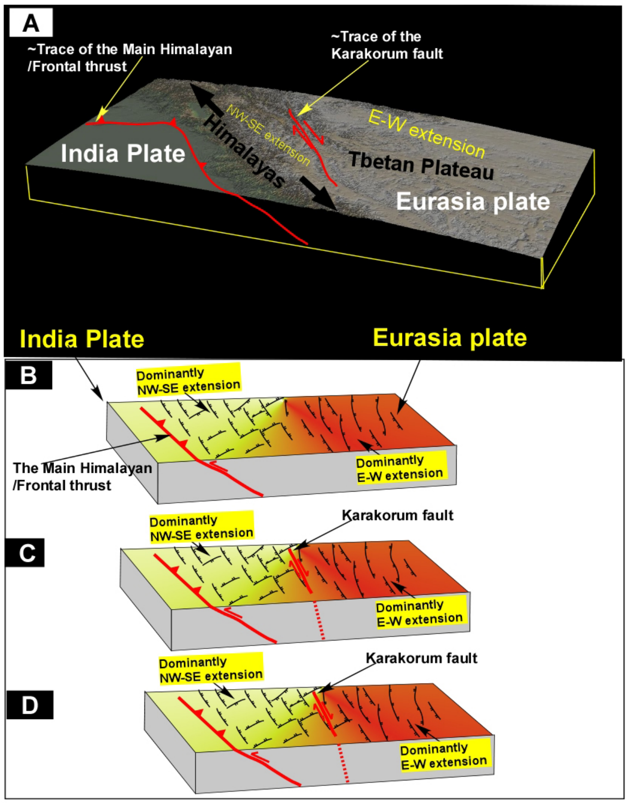

Figure 6: (A) 3-D view of the satellite image shows the two major active fault systems in the NW Himalaya that are reflective of the oblique tectonic convergence between India and Eurasia. The illustrations (B to D) summarize the formation and possible evolution of normal faulting in the studied region. (B) The normal faults could have formed earlier or syntectonic with the oblique plate convergence. (C) This could have later formed strike-slip faults, which have displaced normal faults. (D) This could mean that the Karakorum fault has formed later than normal faults. However, the regional oblique plate tectonic convergence could form both the fault systems together in the region with some time lag between their development history, which seems a normal procedure during the mountain building processes.

parallel and orthogonal normal faulting and strike-slip faulting, where rocks are transported towards ~SE. This has been illustrated (Fig. 6) through a number of 3D illustrations (Fig. 6B–D) to discuss the evolution of normal faulting in the studied region. The faults were formed in response to the collision of lithospheric plates of India and Eurasia (Fig. 6B). This could have formed both, the normal and the strike-slip faults (Fig. 6C). However, the cross cutting relationship between normal and strike-slip faults suggest that some mapped normal faults are truncated by strike-slip faulting, which could indicate that Karakoram fault has formed later than normal faulting (Fig. 6D).

5. Conclusions

The geomorphic expression of faulting that is mapped here shows that ongoing regional deformation is actively contributing towards the ~NW-SE directed crustal extension in the interior of the Himalayas. This is similar to structures that have been mapped in Tibet and the Kashmir Himalayas. The mapped faults are active and are interpreted to have formed in response to the tectonic convergence between the Indian and Eurasian plate. The active nature of deformation suggests distributed deformation in the NW Himalayan and confirms that a portion of tectonic convergence is compensated along regional scale normal faults. It shows that the presence of crustal extension in the interior Himalaya is mainly reflected by the regional normal faulting, which is in contrast to strike-slip and normal faulting in Tibet. The deformation in the interior portions during collisional mountain building processes seems to question the out-of-sequence faulting where such deformation is not a predictable mechanism to release crustal strain. The cause of extension could be related to the ongoing oblique plate convergence where active strike-slip faults transport rocks towards ~SE and we interpret that such faults are expected to slip more towards the east of KF, and less towards the west of it because of the dense network of linked transtensional structures (e.g. major strike-slip and normal faults). This is possibly the reason for low seismic activity on normal and strike slip faults in the Kashmir Himalayas.

6. References

Bilham, R. (2019). Himalayan earthquakes: a review of historical seismicity and early 21st century slip potential. Geological Society, London, Special Publications 483, 423–482. https://doi.org/10.1144/SP483.16.

Burg, J. P., and Bouilhol, P. (2019). Timeline of the South Tibet–Himalayan belt: the geochronological record of subduction, collision, and underthrusting from zircon and monazite U–Pb ages. Canadian Journal of Earth Sciences 56(12), 1318–1332. https://doi.org/10.1139/cjes-2018-0174.

McCaffrey, R., and Nabelek, J. (1998). Role of oblique convergence in the active deformation of the Himalayas and southern Tibet plateau. Geology 26(8), 691–694. https://doi.org/10.1130/0091-7613(1998)026<0691:ROOCIT>2.3.CO;2.

Malik, J.N. and Nakata, T (2003). Active faults and related Late Quaternary deformation along the northwestern Himalayan Frontal Zone. Indian Annals of Geophysics 46, 917–936. https://doi.org/10.4401/ag-3462.

Murphy, M. A., Yin, A., Kapp, P., Harrison, T. M., Manning, C. E., Ryerson, F. J., and Jinghui, G. (2002). Structural evolution of the Gurla Mandhata detachment system, southwest Tibet: Implications for the eastward extent of the Karakoram fault system. Geological Society of America Bulletin 114(4), 428–447. https://doi.org/10.1130/0016-7606(2002)114<0428:SEOTGM>2.0.CO;2.

Nakata, T. (1989). Active faults of the Himalaya of India and Nepal. Geological Society of America Special Publication 232, 243–264. https://doi.org/10.1130/SPE232-p243.

Sahoo, S. and Malik, J. N. (2017). Active fault topography along Kangra Valley Fault in the epicentral zone of 1905 Mw7. 8 earthquake NW Himalaya, India. Quaternary International 462, 90–108. https://doi.org/10.1016/j.quaint.2017.03.020.

Shah, A. (2016). The Kashmir Basin fault and its influence on fluvial flooding in the Kashmir Basin, NW Himalaya. Geological Society of America Special Paper 520, 321–334. https://doi.org/10.1130/2016.2520(28).

Shah, A. A., and Malik, J. N. (2017). Four major unknown active faults identified, using satellite data, in India and Pakistan portions of NW Himalaya. Natural Hazards 88(3), 1845–1865. https://doi.org/10.1007/s11069-017-2949-5.

Shah, A. A., Addly, A. A. B. M., and Samat, M. I. B. A. (2018). Geomorphic Mapping Reveals~ NW-SE Extension in NW Himalaya. In: Kallel A., Erguler, Z. A., Cui, Z.-D., Karrech, A. and Karakus, M. (eds) Recent Advances in Geo-Environmental Engineering, Geomechanics and Geotechnics, and Geohazards. Proceedings of the 1st Springer Conference of the Arabian Journal of Geosciences. Springer, Cham, 385–389. https://doi.org/10.1007/978-3-030-01665-4_89.

Shah, A. A. , Abd Manan, N., Aliudin, N. A. B., Cahyaningsih, C., Batmanathan, N. M. and Malik, J. N. (2020) Formation, Rotation, and Present-Day Configuration of Kashmir and Peshawar Basins in NW Himalaya. Frontiers in Earth Sciences 8:569771. https://doi.org/10.3389/feart.2020.569771.

Shah, A.A., (2013). Earthquake geology of Kashmir Basin and its implications for future large earthquakes. International Journal of Earth Sciences 102, 1957–1966. https://doi.org/10.1007/s00531-013-0874-8.

Stevens, V. L., and Avouac, J. P. (2015). Interseismic coupling on the main Himalayan thrust. Geophysical Research Letters 42(14), 5828-5837. https://doi.org/10.1002/2015GL064845.

Tapponnier, P., and Molnar, P. (1977). Active faulting and tectonics in China. Journal of Geophysical Research 82(20), 2905–2930. https://doi.org/10.1029/JB082i020p02905.

Tapponnier, P., Peltzer, G., Le Dain, A.Y., and Armijo, R. (1982). Propagating extrusion tectonics in Asia: New insights from simple experiments with plasticine. Geology 10, 611–616. https://doi.org/10.1130/0091-7613(1982)10<611:PETIAN>2.0.CO;2.

Yin, A. (2006). Mode of Cenozoic east-west extension in Tibet suggesting a common origin of rifts in Asia during the Indo-Asian collision. Journal of Geophysical Research: Solid Earth 105, 21745–21759. https://doi.org/10.1029/2000JB900168.

Yin, A., and Harrison, T.M. (2000). Geologic evolution of the Himalayan-Tibetan orogen. Annual Review of Earth and Planetary Sciences 28, 211–280. https://doi.org/10.1146/annurev.earth.28.1.211.

Zhao, L. S., and Xie, J. (1993). Lateral variations in compressional velocities beneath the Tibetan Plateau from P_n traveltime tomography. Geophysical Journal International 115(3), 1070–1084. https://doi.org/10.1111/j.1365-246X.1993.tb01510.x.